


Article

Numerical Investigation of Multiple Solutions for Caputo Fractional-Order-Two Dimensional Magnetohydrodynamic Unsteady Flow of Generalized Viscous Fluid over a Shrinking Sheet Using the Adams-Type Predictor-Corrector Method

Liaquat Ali Lund ^{1,2}, Zurni Omar ¹, Sayer O. Alharbi ³, Ilyas Khan ^{4,*} and Kottakkaran Soopy Nisar ⁵

¹ School of Quantitative Sciences, Universiti Utara Malaysia, 06010 Sintok, Kedah

² KCAET Khairpur Mir's Sindh Agriculture University, Tandojam Sindh 70060, Pakistan

³ Department of Mathematics, College of Science Al-Zulfi, Majmaah University, Al-Majmaah 11952, Saudi Arabia

⁴ Faculty of Mathematics and Statistics, Ton Duc Thang University, Ho Chi Minh City 758307, Vietnam

⁵ Department of Mathematics, College of Arts and Science, Prince Sattam bin Abdulaziz University, Wadi Al-Dawaser 11991, Saudi Arabia

* Correspondence: ilyaskhan@tdtu.edu.vn

Received: 29 April 2019; Accepted: 13 June 2019; Published: 27 August 2019



Abstract: In this paper, magnetohydrodynamic (MHD) flow over a shrinking sheet and heat transfer with viscous dissipation has been studied. The governing equations of the considered problem are transformed into ordinary differential equations using similarity transformation. The resultant equations are converted into a system of fractional differential boundary layer equations by employing a Caputo derivative which is then solved numerically using the Adams-type predictor-corrector method (APCM). The results show the existence of two ranges of solutions, namely, dual solutions and no solution. Moreover, the results indicate that dual solutions exist for a certain range of specific parameters which are in line with the results of some previously published work. It is also observed that the velocity boundary layer decreases as the suction and magnetic parameters increase.

Keywords: APCM; Caputo derivative; dual solutions; unsteady flow; MHD; shrinking surface

1. Introduction

The theory of fluid flow on a shrinking surface has numerous applications in real-life problems, such as shrinking film. Additionally, it has capillary effects in small pores, the shrinking-swell behavior of a rising shrinking balloon, and hydraulic properties of agricultural clay soils [1], fuel-cells [2,3], porous materials [4,5], and petroleum engineering [6,7]. Viscous fluid on a shrinking surface has been examined for the first time by Miklavčič and Wang [8], and they discovered that the flow over a shrinking surface did not exist unless sufficient mass suction was applied. It is worth mentioning that the fluid flow on shrinking and stretching surfaces have different characteristics. Gupta et al. [9] examined the magnetohydrodynamic (MHD) flow of micropolar fluid on a shrinking surface with the effect of mixed convection parameter. Meanwhile, Naveed et al. [10] considered the MHD flow of viscous fluid on a curved shrinking sheet. In order to model this problem, a curvilinear coordinates system was employed and the dual solutions were obtained. The MHD flow of nanofluid over a nonlinear stretching/shrinking wedge was considered by Khan et al. [11]. Soid et al. [12] investigated the unsteady MHD stagnation point flow over a shrinking surface and found dual solutions. Likewise,

Zaib et al. [13] considered the unsteady flow of the Williamson nanofluid over a shrinking surface and found dual solutions by using the shooting method. Lund et al. [14] analyzed the Darcy–Forchheimer flow of the Casson nanofluid with the impact of the slip condition on the shrinking surface and expressed that the existence of dual solutions relies upon the suction parameter. The slip effects on the nanofluid by utilizing the Buongiorno model has been examined by Dero et al. [15]. They found dual solutions by implementations of the shooting method and stated that it was due to the unsteadiness of the parameter. Similarly, Alarifi et al. [16] considered the stagnation point flow and found dual solutions for an opposing case. Triple solutions of micropolar nanofluid over a shrinking surface have been obtained by employing the shooting method [17]. Moreover, Lund et al. [18] performed a stability analysis by using the three-stage Lobatto IIIa formula and concluded only first solution to be stable. To the best of our knowledge, most of the studies and investigations of fluid flow have not used the Caputo fractional derivatives for multiple solutions. Therefore, the main objective of this work is to consider Caputo fractional derivatives, solve the governing equations by using the Adams-type predictor-corrector method, and find multiple solutions.

From published literature, it can be concluded that the possibility of the existence of multiple solutions of boundary layer flow on a shrinking surface is greater than on a stretching sheet. It is also discovered that the solution of fluid flow over a shrinking surface is possible only in the presence of high suction [19]. In other words, the solution is possible only on permeable surfaces. According to Mishra et al. [20], multiple solutions depend on the non-linearity in governing equations of fluid flow and other factors. Moreover, the existence of multiple solutions also depends on the values of different physical parameters such as magnetic, Reynold numbers, Prandtl numbers, and suction parameters, as claimed by Schlichting [21]. This claim complies with the findings of other researchers who discovered that the ranges of multiple solutions, single solutions, and no solutions depend on the values, such as the magnetic parameter [18], suction parameter [14], and surface velocity parameter [22]. Fang and Zhang [23] examined the steady MHD flow of viscous fluid over a shrinking surface and found dual solutions analytically. They concluded that dual and single solutions exist when $0 < M < 1$ and $M \geq 1$, respectively. Previous researchers attempted to determine multiple solutions using various analytical and numerical methods. Rana et al. [24] used the homotopy analysis method to find the multiple solutions. Rohni et al. [25] and Ishak et al. [26] found multiple solutions by using the Keller-box method. Fang et al. [27] employed an analytical approach to find multiple solutions of viscous fluid in exact form and Raza et al. [28] considered the shooting method with the Runge–Kutta of the fourth order method to find the multiple solutions of fluid flow. The objective of this paper is to extend the work of Fang and Zhang [23] under the consideration of unsteady flow and heat equation with viscous dissipation using the new approach with the Caputo derivative to reduce the governing equations to the first order ordinary differential equations, which are then solved by the Adams-type predictor-corrector method.

The MHD field was initiated by Hannes Alfvén (1908–1995) who was a famous Swedish physicist. Interest in the MHD flow started to gain attention when Hartmann invented the electromagnetic pump in 1918 [29]. In recent years, the study of non-uniform transverse-magnetic field effects is applied in many engineering problems. For example, electrically-conducting fluids that flow along with magnetic field have significant applications in oil exploration, cooling nuclear reactors, boundary layer control in the aerodynamics field, extraction of geothermal energy, and MHD generators and plasma studies. Due to the important applications of MHD flow, many researchers, mathematicians, and engineers considered MHD flow-related problems in their studies [30–32]. Ellahi et al. [33] considered the effect of MHD on Couple Stress Fluid. Makinde et al. [34] examined nanofluid under the influence of MHD and found that the hydrodynamic boundary layer is a decreasing function for higher values of magnetic parameters. This article is presented as follows: Section 2 discusses the problem formulation, in which governing equations are derived, and also gives some useful definitions and properties using solution methodology. In Section 3, numerical are presented numerically and graphically. Finally, Section 4 concludes this study by giving key findings and remarks.

2. Problem Formulation

2.1. Boundary Layer Governing Equations

The MHD flow of two-dimensional incompressible viscous fluid over a continuously unsteady shrinking surface is considered. The velocity of mass transfer and the shrinking surface are assumed to be $v_w(x, t)$ and $u_w(x, t)$, respectively, where t is the time and x is the coordinate measured with the shrinking surface. Under these assumptions with viscous dissipation, the governing Navier–Stokes (NS) equations of this problem are given by:

$$\frac{\partial u}{\partial x} + \frac{\partial v}{\partial y} = 0 \quad (1)$$

$$\frac{\partial u}{\partial t} + u \frac{\partial u}{\partial x} + v \frac{\partial u}{\partial y} = -\frac{1}{\rho} \frac{\partial P}{\partial x} + \nu \left(\frac{\partial^2 u}{\partial x^2} + \frac{\partial^2 u}{\partial y^2} \right) - \frac{\sigma^* B^2 u}{\rho} \quad (2)$$

$$\frac{\partial v}{\partial t} + u \frac{\partial v}{\partial x} + v \frac{\partial v}{\partial y} = -\frac{1}{\rho} \frac{\partial P}{\partial y} + \nu \left(\frac{\partial^2 v}{\partial x^2} + \frac{\partial^2 v}{\partial y^2} \right) \quad (3)$$

$$\frac{\partial T}{\partial t} + u \frac{\partial T}{\partial x} + v \frac{\partial T}{\partial y} = \alpha \left(\frac{\partial^2 T}{\partial x^2} + \frac{\partial^2 T}{\partial y^2} \right) + \frac{\mu}{\rho c_p} \left[\left(\frac{\partial u}{\partial x} \right)^2 + \left(\frac{\partial u}{\partial y} \right)^2 \right] \quad (4)$$

Subject to the following boundary conditions:

$$t < 0: u = v = 0, T = T_\infty \text{ for all } x; y$$

$$t \geq 0: u = u_w(x, t) = -\frac{cx}{1-\gamma t}, v = v_w(x, t) = -\sqrt{\frac{\nu f c}{1-\gamma t}} f(0) = S, T = T_w(x, t) = T_\infty + \frac{bx^m}{1-\gamma t} \text{ at } y = 0$$

$$u \rightarrow 0; T \rightarrow T_\infty \text{ as } y \rightarrow \infty \quad (5)$$

where the pressure of fluid is denoted by P , velocity components along the x and y directions are represented by u and v , respectively, temperature of fluid is T , kinematic viscosity of the fluid is ν , density of the fluid is ρ , thermal diffusivity of the fluid is α , $B = \frac{B_0}{(1-\gamma t)^{1/2}}$ is the transverse magnetic field of strength which is applied with the normal surface direction, and b , c , and m are all positive constants. It is worth mentioning that $m = 1$ and $m = 0$ indicate linear and constant variation with x of the wall of temperature, respectively.

Now, we introduce the similarity variables for Equations (1)–(5) as follows:

$$u = \frac{cx}{(1-\gamma t)} f'(\eta); v = -\sqrt{\frac{cv}{(1-\gamma t)}} f(\eta), \theta(\eta) = \frac{T - T_\infty}{T_w - T_\infty} \quad (6)$$

Substituting (6) into Equations (2)–(4) yields the following system of ordinary differential equations

$$f''' + ff'' - (f')^2 - A \left(\frac{\eta}{2} f'' + f' \right) - Mf' = 0 \quad (7)$$

$$\frac{1}{Pr} \theta'' + f\theta' - m f' \theta - A \left(\frac{\eta}{2} \theta' + \theta \right) + Ec(f'')^2 = 0 \quad (8)$$

with reduced boundary conditions

$$f(0) = S; f'(0) = -1; \theta(0) = 1$$

$$f'(\eta) \rightarrow 0; \theta(\eta) \rightarrow 0 \text{ as } \eta \rightarrow \infty \quad (9)$$

where $A = \frac{\gamma}{c}$ is the unsteadiness parameter, $M = \frac{\sigma(B_0)^2}{\rho c}$ is the magnetic parameter, $Ec = \frac{U_w^2}{C_p(T_w - T_\infty)}$ is the Eckert number, and $Pr = \frac{\beta}{\alpha}$ is the Prandtl number. In our problem, we consider a decelerating shrinking surface ($A < 0$) as assumed in [35,36].

2.2. Preliminaries on the Caputo Fractional Derivatives

In this section, the definition of the Caputo fractional derivative and its main properties are introduced.

Definition 1. Let $t > a, a > 0, a, \alpha, t \in \mathfrak{R}$. The Caputo fractional derivative of the order α of function $f \in C^n$ is expressed as:

$${}_a^C D_t^\alpha f(t) = \frac{1}{\Gamma(n - \alpha)} \int_a^t \frac{f^{(n)}(\xi)}{(t - \xi)^{\alpha + 1 - n}} d\xi, \quad n - 1 < \alpha < n \in N \tag{10}$$

Property 1. Let $f(t), g(t) : [a, b] \rightarrow \mathfrak{R}$ be such that ${}_a^C D_t^\alpha f(t)$ and ${}_a^C D_t^\alpha g(t)$ exist almost everywhere, and let $c_1, c_2 \in \mathfrak{R}$. Then ${}_a^C D_t^\alpha \{c_1 f(t) + c_2 g(t)\}$ exists almost everywhere and

$${}_a^C D_t^\alpha \{c_1 f(t) + c_2 g(t)\} = c_1 {}_a^C D_t^\alpha f(t) + c_2 {}_a^C D_t^\alpha g(t) \tag{11}$$

Property 2. If $f(t) = c$ is a constant function then the fractional derivative of the function is equal to 0, and mathematically it can be expressed as:

$${}_a^C D_t^\alpha c = 0 \tag{12}$$

We considered the general fractional differential equation involving the Caputo derivative below

$${}_a^C D_t^\alpha x(t) = f(t, x(t)), \quad \alpha \in (0, 1) \tag{13}$$

with initial conditions $x_0 = x(t_0)$.

Definition 2. The constant x^* is an equilibrium point of the Caputo fractional dynamic system (13) if, and only if, $f(t, x^*) = 0$.

Here, we introduce the new fractional Atangana–Baleanu derivatives along the non-local and non-singular kernel [37,38].

Definition 3. Let $f \in H^1(a, b), b > a, \alpha \in [0, 1]$, then the new fractional derivatives of the Caputo behavior can be expressed as:

$$D_t^\alpha (f(t)) = \frac{B(\alpha)}{1 - \alpha} \int_a^t f(x) \exp\left(-\alpha \frac{t - x}{1 - \alpha}\right) dx$$

where $B(\alpha)$ denotes a normalization function obeying $B(0) = B(1) = 1$.

In the case when the function does not belong to $H^1(a, b)$, the derivative is given by

$$D_t^\alpha (f(t)) = \frac{\alpha B(\alpha)}{1 - \alpha} \int_a^t (f(t) - f(x)) \exp\left(-\alpha \frac{t - x}{1 - \alpha}\right) dx$$

Furthermore, if $\sigma = \frac{1 - \alpha}{\alpha} \in [0, \infty)$, and $\alpha = \frac{1}{1 + \sigma} \in [0, 1]$, then the above Equation becomes

$$D_t^\sigma (f(t)) = \frac{N(\sigma)}{\sigma} \int_a^t f(x) \exp\left(-\frac{t - x}{\sigma}\right) dx, \quad N(0) = N(\infty) = 1$$

2.3. Solution Methodology

Choosing different variables below

$$y_1 = \eta, y_2 = f, y_3 = f', y_4 = f'', y_5 = \theta, y_6 = \theta' \tag{14}$$

Equations (7) and (8) can be transformed into a system of first-order differential equations. Then, the Caputo fractional-order derivative is applied to the resultant system to produce a fractional-order system of the following form:

$$\begin{cases} D_{\eta}^{\alpha}y_1 = 1, D_{\eta}^{\alpha}y_2 = y_3, D_{\eta}^{\alpha}y_3 = y_4; D_{\eta}^{\alpha}y_4 = (y_3)^2 - y_2y_4 + A\left(y_3 + \frac{y_1y_4}{2}\right) + My_3 \\ D_{\eta}^{\alpha}y_5 = y_6, D_{\eta}^{\alpha}y_6 = Pr\left\{my_3y_5 - y_2y_6 + A\left(y_5 + \frac{y_1y_6}{2}\right) - Ec(y_4)^2\right\} \end{cases} \tag{15}$$

with boundary conditions below:

$$y_1 = 0, y_2 = S, y_3 = -1, y_4 = u_1, y_5 = 1, y_6 = u_2 \tag{16}$$

Now, the Adams types predictor-corrector method has been applied to get the solution of fractional differential equations. The error of this method is of the order h^5 , where h is the grid size.

3. Results and Discussion

The governing Equation (15) with initial conditions (16) is solved using the Adams-type predictor-corrector method, and dual solutions are found depending on the suction parameter. It is worth mentioning that when an unsteady parameter is equal to 0, our equation of momentum is reduced to an equation obtained in [23], which is the major reference of our work. Furthermore, the results of the coefficient of skin friction in our problem are in good agreement with their work. According to our results, the coefficient of skin friction is equal to $f''(0) = \frac{S \pm \sqrt{S^2 - 4 + 4M}}{2}$. For details on the comparison, please refer to Table 1. From the table, we can conclude that only the first solution of our problem is a physical realizable solution, since $f''(0) > 0$, whereas the second solution is unstable because most of the values of $f''(0)$ are less than 0. It is worth mentioning that our results of the first solution are approximately equal to the result of a published article [23], which gives us confidence on our calculation (see Table 1). It should be noted that if $\alpha < 1$, multiple solutions do not exist and do not fulfill the boundary conditions asymptotically.

Table 1. Comparison $f''(0)$ of present results with [23].

M	S	Fang	Zhang [23]	Present	Results
		1st Solution	2nd Solution	1st Solution	2nd Solution
0.5	3	2.8228756	0.1771243	2.8203848	-0.3554574
	2	1.7071067	0.2928932	1.7063214	0.2845535
0	3	2.6180339	0.3819660	2.6165735	-0.2181474
	2	1	1	1.0019038	0.94503648

Figure 1 shows the effect of the suction parameter on the velocity profile. It was noticed that the thickness of the velocity boundary layer decreased as suction increased in the first solution. This occurred due to the fact that high suction produced the resistance in the fluid flow, and, as a result, the velocity and thickness of the momentum boundary layer decreased. On the other hand, the suction was proportional to the velocity profile in the second solution.

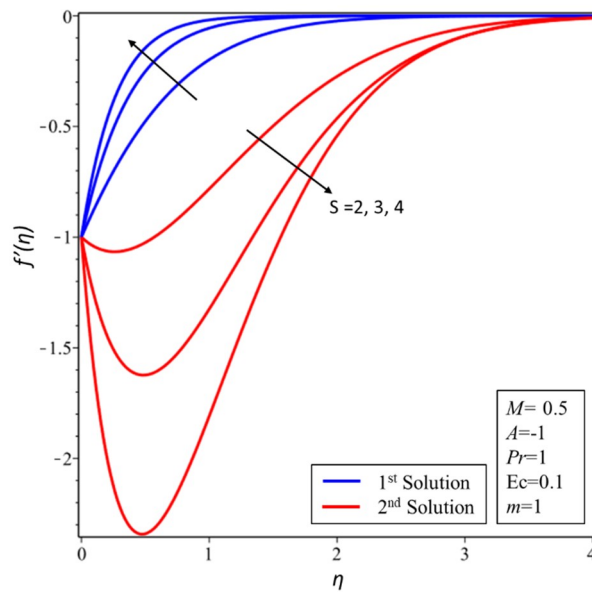


Figure 1. $f'(\eta)$ for increasing values of S .

The effect of the magnetic parameter M on the velocity is demonstrated in Figure 2. The velocity of the fluid flow decreased as magnetic parameter M increased in the first solution, as expected. This was due to the Lorentz or electromagnetic force, which can be defined as “the force which is exerted by a magnetic field on a moving fluid” [39]. We can say this force opposes the transport phenomenon. However, the opposite trend can be seen in the second solution.

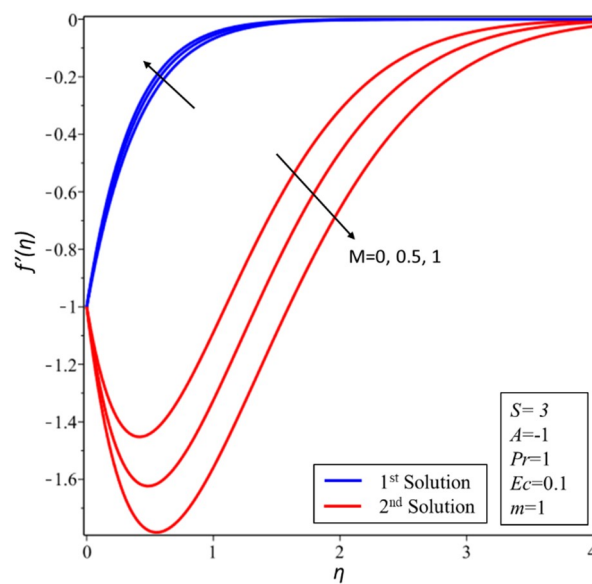


Figure 2. $f'(\eta)$ for increasing values of M and $\alpha = 1$.

Based on the results shown in Figure 3, there no change was noticed in the first solution when the magnitude of the unsteadiness parameter increased. On the other hand, the velocity layer became thicker initially and then thinner in the second solution, since deaccelerating of the unsteadiness parameter produced more drag force, which caused the thickness of the momentum boundary layer to decrease.

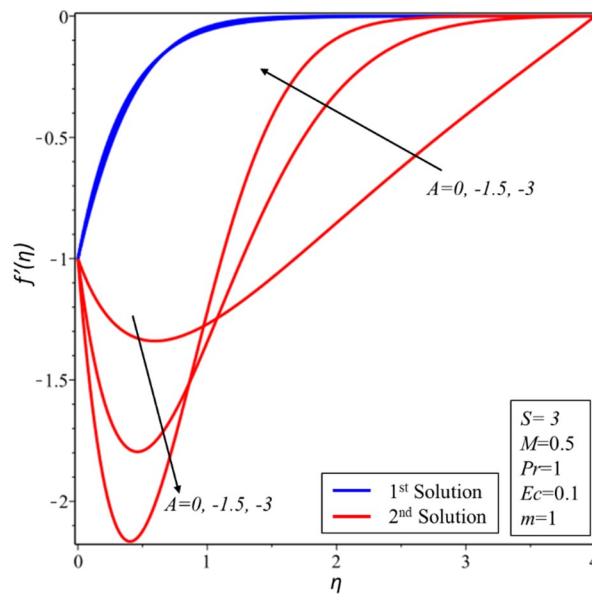


Figure 3. $f'(\eta)$ for increasing values of A and $\alpha = 1$.

The effect of the unsteadiness parameter A on a dimensionless profile of temperature is depicted in Figure 4. Both thermal boundary layer thicknesses and temperatures decreased initially and then started to increase when the unsteadiness parameter A was increased in the second solution. This behavior was expected because the momentum boundary layer declined and, therefore, the temperature increased. However, no difference could be seen in the first solution with the increasing magnitude of the unsteadiness parameter A .

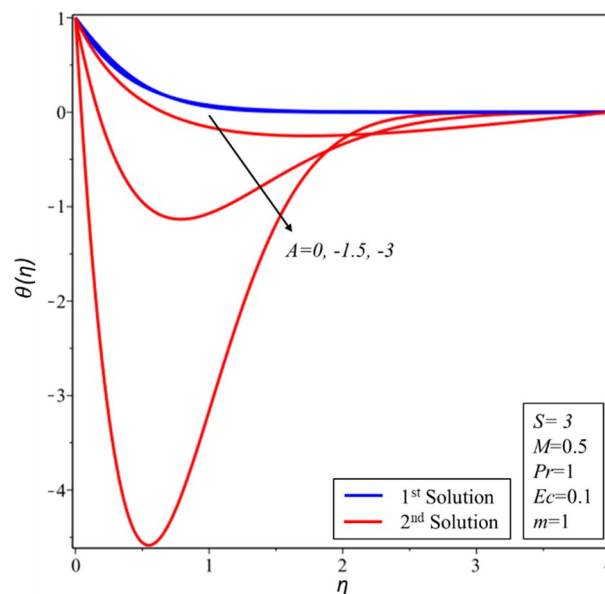


Figure 4. $\theta(\eta)$ for increasing values of A and $\alpha = 1$.

Figure 5 was drawn for the Prandtl number effect Pr on the profile of temperature. We can see that the temperature declined with respect to $Pr = 0.04$ to 6.7 in the first solution. This was because “fluid has relatively lower thermal conductivity for a large value of Prandtl number, which decreases the conduction and thickness of the thermal boundary layer” [40], and, consequently, the temperature reduced. This was because the “Prandtl number Pr which is the ratio of momentum diffusion to thermal” [18]. On the other hand, the thermal boundary layer thickness and temperature increase in the range of $0.04 \leq Pr \leq 3$ decreased in the range of $3 \leq Pr \leq 6.7$ in the second solution.

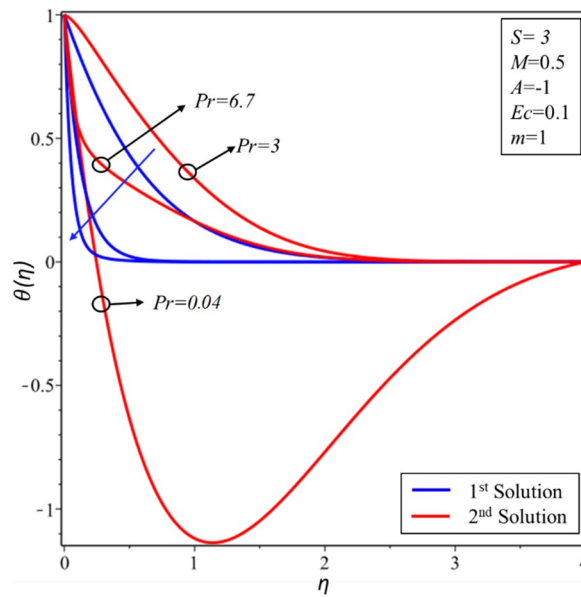


Figure 5. $\theta(\eta)$ for increasing values of Pr and $\alpha = 1$.

Figure 6 indicates the temperature increase when the Eckert number was increased in the first solution. This was due to fact that an expansion in dissipation enhanced the flow of thermal conductivity, which extended the temperature and thermal boundary layer thickness. On the other hand, the Eckert number was inversely proportional to the temperature and thickness of the thermal boundary layer in the second solution.

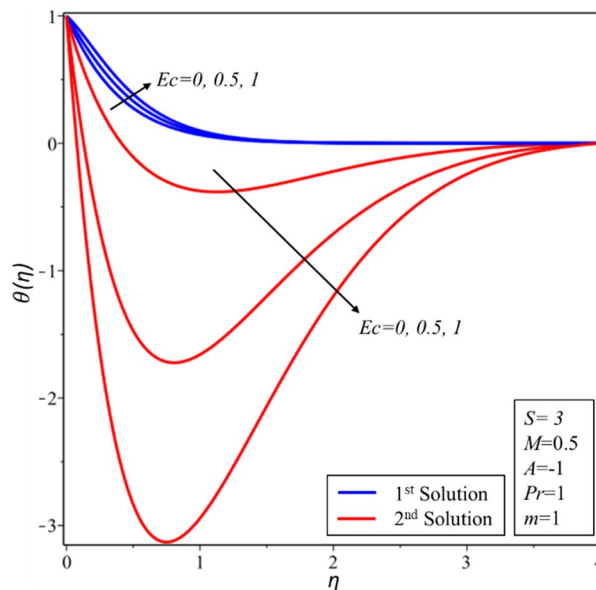


Figure 6. $\theta(\eta)$ for increasing values of Ec and $\alpha = 1$.

The graph of the coefficient of skin friction for several values of S and different values of A is illustrated in Figure 7. It was observed that the skin friction coefficient increased (decreased) when suction was increased (reduced) in the first (second) solution. However, it decreased with the decreasing of the unsteady parameter A . Physically, resistance occurred due to increments in the suction parameter in the stable solution, while the opposite trend was seen in the unstable solution.

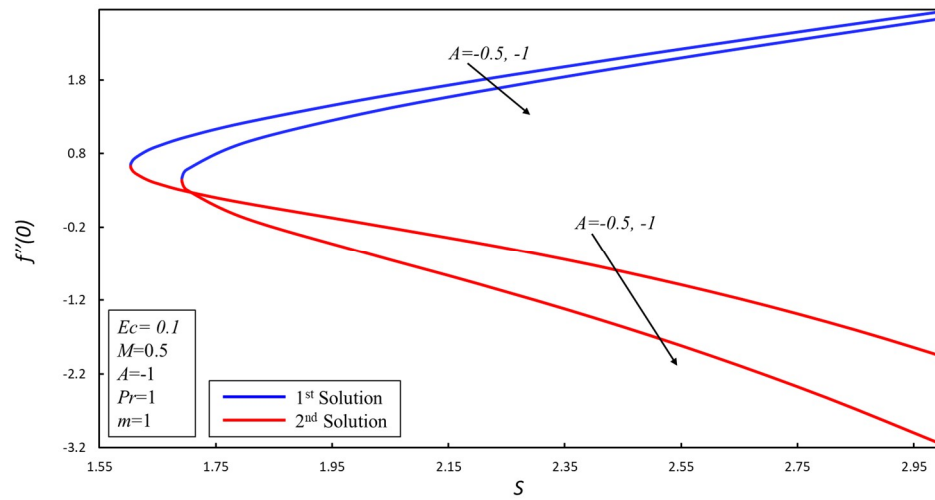


Figure 7. Coefficient of skin friction for different values of A .

Figure 8 shows the effect of α on the profile of the temperature. It was noticed that multiple solutions were difficult to be obtained when $\alpha < 1$. As α increased, the temperature of the fluid increased in the first solution and decreased in the second solution.

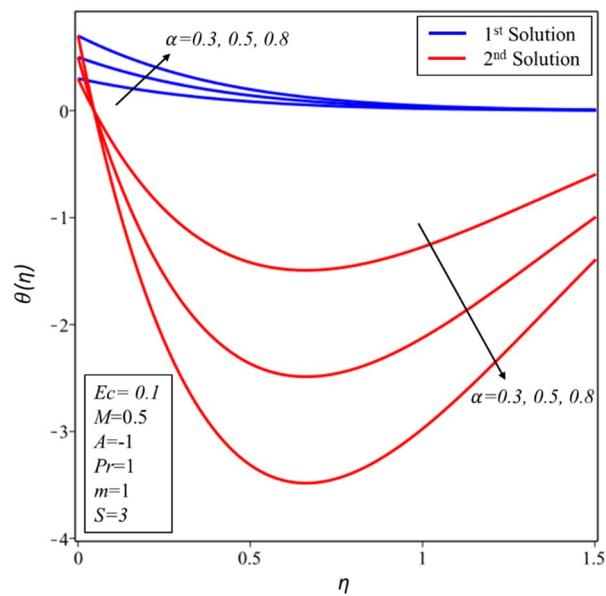


Figure 8. $\theta(\eta)$ for increasing values of α .

Figure 9 demonstrates the effect of α on the velocity profile. In both solutions, the velocity of the fluid decreased when α increased.

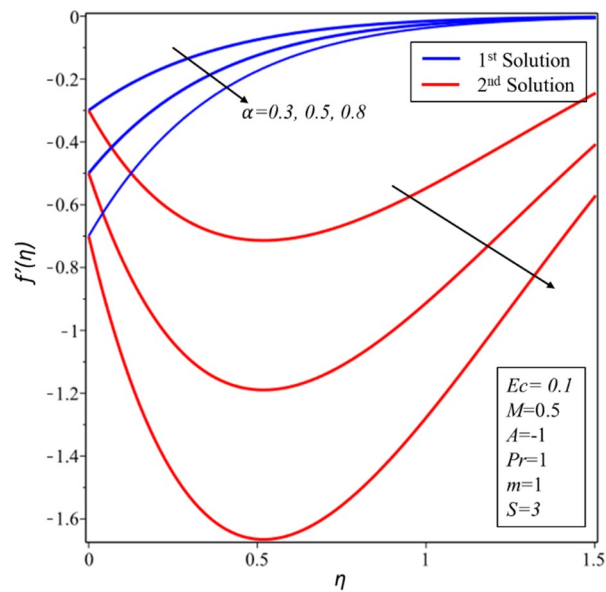


Figure 9. $f'(\eta)$ for increasing values of α .

4. Conclusion Remarks

The magnetohydrodynamic (MHD) flow over a shrinking sheet and heat transfer with viscous dissipation is numerically studied. The governing equations of the momentum and energy are transformed into the ordinary differential equations by using similarity transformation. The resultant equations have been transformed into a system of fractional differential equations by using the Caputo derivative. Fractional differential boundary layer equations, based on Caputo operators, are solved numerically by the Adams-type predictor-corrector method. We compared our result with a past published article and found it in good agreement with the first solution. Further, our results of the second solution did not concur with the published results. This was because of the heat equation and its different parameter effects on the unstable (second) solution. On the other hand, there existed two different ranges, namely, no solution and dual solutions, which depended on the magnetic and suction parameters.

Author Contributions: Z.O. and L.A.L. formulated the problem. L.A.L. and S.O.A. transformed the problem and computed the results. I.K. and K.S.N. discussed the results physically. All the authors equally contributed in writing the manuscript.

Funding: This research received no external funding.

Acknowledgments: The authors would like to thank Deanship of Scientific Research, Majmaah University for supporting this work.

Conflicts of Interest: The authors declare no conflict of interest.

References

1. Rohni, A.M.; Ahmad, S.; Pop, I. Flow and heat transfer at a stagnation-point over an exponentially shrinking vertical sheet with suction. *Int. J. Therm. Sci.* **2014**, *75*, 164–170. [[CrossRef](#)]
2. Xiao, B.; Wang, W.; Zhang, X.; Long, G.; Chen, H.; Cai, H.; Deng, L. A novel fractal model for relative permeability of gas diffusion layer in proton exchange membrane fuel cell with capillary pressure effect. *Fractals* **2019**, *27*, 1950012. [[CrossRef](#)]
3. Liang, M.; Liu, Y.; Xiao, B.; Yang, S.; Wang, Z.; Han, H. An analytical model for the transverse permeability of gas diffusion layer with electrical double layer effects in proton exchange membrane fuel cells. *Int. J. Hydrog. Energy* **2018**, *43*, 17880–17888. [[CrossRef](#)]

4. Xiao, B.; Wang, W.; Zhang, X.; Long, G.; Fan, J.; Chen, H.; Deng, L. A novel fractal solution for permeability and Kozeny-Carman constant of fibrous porous media made up of solid particles and porous fibers. *Powder Technol.* **2019**, *349*, 92–98. [[CrossRef](#)]
5. Liang, M.; Fu, C.; Xiao, B.; Luo, L.; Wang, Z. A fractal study for the effective electrolyte diffusion through charged porous media. *Int. J. Heat Mass Transf.* **2019**, *137*, 365–371. [[CrossRef](#)]
6. Long, G.; Liu, S.; Xu, G.; Wong, S.W.; Chen, H.; Xiao, B. A perforation-erosion model for hydraulic-fracturing applications. *SPE Prod. Oper.* **2018**, *33*, 770–783. [[CrossRef](#)]
7. Long, G.; Xu, G. The effects of perforation erosion on practical hydraulic-fracturing applications. *SPE J.* **2017**, *22*, 645–659. [[CrossRef](#)]
8. Miklavčič, M.; Wang, C.Y. Viscous flow due to a shrinking sheet. *Q. Appl. Math.* **2006**, *14*, 283–290. [[CrossRef](#)]
9. Gupta, D.; Kumar, L.; Bég, O.A.; Singh, B. Finite Element Analysis of MHD Flow of Micropolar Fluid over a Shrinking Sheet with a Convective Surface Boundary Condition. *J. Eng. Thermophys.* **2018**, *27*, 202–220. [[CrossRef](#)]
10. Naveed, M.; Abbas, Z.; Sajid, M.; Hasnain, J. Dual solutions in hydromagnetic viscous fluid flow past a shrinking curved surface. *Arab. J. Sci. Eng.* **2018**, *43*, 1189–1194. [[CrossRef](#)]
11. Khan, U.; Ahmed, N.; Mohyud-Din, S.T.; Bin-Mohsin, B. Nonlinear radiation effects on MHD flow of nanofluid over a nonlinearly stretching/shrinking wedge. *Neural Comput. Appl.* **2017**, *28*, 2041–2050. [[CrossRef](#)]
12. Soid, S.K.; Ishak, A.; Pop, I. Unsteady MHD flow and heat transfer over a shrinking sheet with ohmic heating. *Chin. J. Phys.* **2017**, *55*, 1626–1636. [[CrossRef](#)]
13. Zaib, A.; Haq, R.U.; Chamkha, A.J.; Rashidi, M.M. Impact of nonlinear radiative nanoparticles on an unsteady flow of a Williamson fluid towards a permeable convectively-heated shrinking sheet. *World J. Eng.* **2018**, *15*, 731–742. [[CrossRef](#)]
14. Lund, L.A.; Omar, Z.; Khan, I.; Raza, J.; Bakouri, M.; Tlili, I. Stability analysis of Darcy-Forchheimer flow of Casson type nanofluid over an exponential sheet: Investigation of critical points. *Symmetry* **2019**, *11*, 412. [[CrossRef](#)]
15. Dero, S.; Uddin, M.J.; Rohni, A.M. Stefan blowing and slip effects on unsteady nanofluid transport past a shrinking sheet: Multiple solutions. *Heat Transf.—Asian Res.* **2019**, *48*, 1149–1544. [[CrossRef](#)]
16. Alarifi, I.M.; Abokhalil, A.G.; Osman, M.; Lund, L.A.; Aayed, M.B.; Belmabrouk, H.; Tlili, I. MHD flow and heat transfer over vertical stretching sheet with heat sink or source effect. *Symmetry* **2019**, *11*, 297. [[CrossRef](#)]
17. Dero, S.; Rohni, A.M.; Saaban, A. MHD micropolar nanofluid flow over an exponentially stretching/shrinking surface: Triple solutions. *J. Adv. Res. Fluid Mech. Therm. Sci.* **2019**, *56*, 165–174.
18. Lund, L.A.; Omar, Z.; Khan, I. Analysis of dual solution for MHD flow of Williamson fluid with slippage. *Heliyon* **2019**, *5*, e01345. [[CrossRef](#)]
19. Bhattacharyya, K.; Banerjee, A.; Zaib, A.; Mahato, S.K. MHD mixed convection flow of a non-Newtonian Powell-Eyring fluid over a permeable exponentially shrinking sheet. *FHMT* **2018**, *10*, 30. [[CrossRef](#)]
20. Mishra, S.; DebRoy, T. A computational procedure for finding multiple solutions of convective heat transfer equations. *J Phys. D Appl. Phys.* **2005**, *38*, 2977. [[CrossRef](#)]
21. Schlichting, H. *Boundary-Layer Theory*; McGraw-Hill: New York, NY, USA, 1968.
22. Rahman, M.M.; Rosca, A.V.; Pop, I. Boundary layer flow of a nanofluid past a permeable exponentially shrinking surface with convective boundary condition using Buongiorno's model. *Int. J. Numer. Methods Heat Fluid Flow* **2015**, *25*, 299–319. [[CrossRef](#)]
23. Fang, T.; Zhang, J. Closed-form exact solutions of MHD viscous flow over a shrinking sheet. *Commun. Nonlinear Sci. Numer. Simul.* **2009**, *14*, 2853–2857. [[CrossRef](#)]
24. Rana, P.; Shukla, N.; Gupta, Y.; Pop, I. Homotopy analysis method for predicting multiple solutions in the channel flow with stability analysis. *Commun. Nonlinear Sci. Numer. Simul.* **2018**, *66*, 183–193. [[CrossRef](#)]
25. Rohni, A.M.; Ahmad, S.; Pop, I. Boundary layer flow over a moving surface in a nanofluid beneath a uniform free stream. *Int. J. Numer. Methods Heat Fluid Flow* **2011**, *21*, 828–846. [[CrossRef](#)]
26. Ishak, A.; Nazar, R.; Pop, I. Mixed convection boundary layer flow adjacent to a vertical surface embedded in a stable stratified medium. *Int. J. Heat Mass Transf.* **2008**, *51*, 3693–3695. [[CrossRef](#)]
27. Fang, T.; Yao, S.; Zhang, J.; Aziz, A. Viscous flow over a shrinking sheet with a second order slip flow model. *Commun. Nonlinear Sci. Numer. Simul.* **2010**, *15*, 1831–1842. [[CrossRef](#)]

28. Raza, J.; Rohni, A.M.; Omar, Z. Rheology of micropolar fluid in a channel with changing walls: Investigation of multiple solutions. *J. Mol. Liq.* **2016**, *223*, 890–902. [[CrossRef](#)]
29. Mutuku-Njane, W.N. Analysis of Hydromagnetic Boundary Layer Flow and Heat Transfer of Nanofluids. Ph.D. Thesis, Cape Peninsula University of Technology, Cape Town, South Africa, 2014.
30. Sheikholeslami, M.; Ellahi, R. Three dimensional mesoscopic simulation of magnetic field effect on natural convection of nanofluid. *Int. J. Heat Mass Transf.* **2015**, *89*, 799–808. [[CrossRef](#)]
31. Kandelousi, M.S.; Ellahi, R. Simulation of ferrofluid flow for magnetic drug targeting using the lattice Boltzmann method. *Z. Für Naturforschung A* **2015**, *70*, 115–124. [[CrossRef](#)]
32. Zeeshan, A.; Shehzad, N.; Abbas, T.; Ellahi, R. Effects of radiative electro-magnetohydrodynamics diminishing internal energy of pressure-driven flow of Titanium dioxide—Water nanofluid due to entropy generation. *Entropy* **2019**, *21*, 236. [[CrossRef](#)]
33. Ellahi, R.; Zeeshan, A.; Hussain, F.; Abbas, T. Two-phase Couette flow of couple stress fluid with temperature dependent viscosity thermally affected by magnetized moving surface. *Symmetry* **2019**, *11*, 647. [[CrossRef](#)]
34. Makinde, O.D.; Mabood, F.; Khan, W.A.; Tshehla, M.S. MHD flow of a variable viscosity nanofluid over a radially stretching convective surface with radiative heat. *J. Mol. Liq.* **2016**, *219*, 624–630. [[CrossRef](#)]
35. Tie-Gang, F.; Ji, Z.; Shan-Shan, Y. Viscous flow over an unsteady shrinking sheet with mass transfer. *Chin. Phys. Lett.* **2009**, *26*, 014703. [[CrossRef](#)]
36. Rohni, A.M.; Ahmad, S.; Pop, I. Flow and heat transfer over an unsteady shrinking sheet with suction in nanofluids. *Int. J. Heat Mass Transf.* **2012**, *55*, 1888–1895. [[CrossRef](#)]
37. Atangana, A.; Baleanu, D. New fractional derivatives with non-local and non-singular kernel: Theory and application to heat transfer model. *J. Therm. Sci.* **2016**, *20*, 763–769. [[CrossRef](#)]
38. Baleanu, D.; Mousalou, A.; Rezapour, S. On the existence of solutions for some infinite coefficient-symmetric Caputo-Fabrizio fractional integro-differential equations. *Bound. Value Probl.* **2017**, *2017*, 145. [[CrossRef](#)]
39. Sheikholeslami, M.; Chamkha, A.J. Influence of Lorentz forces on nanofluid forced convection considering Marangoni convection. *J. Mol. Liq.* **2017**, *225*, 750–757. [[CrossRef](#)]
40. Lund, L.A.; Omar, Z.; Khan, I.; Dero, S. Multiple solutions of $\text{Cu-C}_6\text{H}_9\text{NaO}_7$ and $\text{Ag-C}_6\text{H}_9\text{NaO}_7$ nanofluids flow over nonlinear shrinking surface. *J. Cent. South Univ.* **2019**, *26*, 1283–1293. [[CrossRef](#)]



© 2019 by the authors. Licensee MDPI, Basel, Switzerland. This article is an open access article distributed under the terms and conditions of the Creative Commons Attribution (CC BY) license (<http://creativecommons.org/licenses/by/4.0/>).